ELSEVIER

Contents lists available at ScienceDirect

Sensors and Actuators: B. Chemical

journal homepage: www.elsevier.com/locate/snb





Investigation of the role of photoacoustic phase in $N_2O(v_3)$ vibrational relaxation rate determination

Yong Wang ^{a,b,1}, Jiapeng Wang ^{a,b,1}, Gang Wang ^{a,b}, Jialiang Dai ^{a,b}, Ruyue Cui ^{a,b}, Chaofan Feng ^c, Mariagrazia Olivieri ^d, Angelo Sampaolo ^{a,d}, Pietro Patimisco ^{a,d}, Vincenzo Spagnolo ^{a,d,*}, Lei Dong ^{a,b,*}, Hongpeng Wu ^{a,b,*}

- a State Key Laboratory of Quantum Optics Technologies and Devices, Institute of Laser Spectroscopy, Shanxi University, Taiyuan 030006, China
- ^b Collaborative Innovation Center of Extreme Optics, Shanxi University, Taiyuan 030006, China
- ^c College of Physics and Electrical Engineering, Shanxi University, Taiyuan 030006, China
- ^d PolySense Lab, Dipartimento Interateneo di Fisica, University and Politecnico of Bari, Via Amendola 173, Bari 70126, Italy

ARTICLE INFO

Keywords: Photoacoustic spectroscopy Nitrous oxide Vibration-translation Relaxation time

ABSTRACT

This study investigates the relaxation dynamics of the ν_3 energy level of nitrous oxide (N₂O) molecules in synthetic air using a 4.5 µm distributed feedback quantum cascade laser (DFB-QCL) combined with photoacoustic spectroscopy (PAS) technique. A comprehensive theoretical model coupling vibration-translation (V-T) relaxation processes and vibration-vibration (V-V) energy transfer was developed, enabling a rigorous theoretical derivation of the system-wide vibrational relaxation time. Through in-depth analysis of photoacoustic signal phase characteristics, the molecular relaxation times of both N₂O (ν_3) (1.6 µs atm) and H₂O (0.33 µs atm) were simultaneously extracted. Thorough cross-validation against literature values demonstrated that photoacoustic phase information serves as a highly sensitive probe for detecting gas molecular energy relaxation processes. This research not only validates the technical feasibility and analytical superiority of PAS phase technology in measuring gas relaxation times but also introduces a novel high-precision spectroscopic analysis method for studying vibrational dynamics in complex molecular systems, showcasing its potential applications in environmental monitoring and molecular dynamics research.

1. Introduction

Nitrous oxide (N_2O) is a potent greenhouse gas with high global warming potential. One unit of N_2O emission is equivalent to 298 units of carbon dioxide (CO_2), making it a significant contributor to climate change and ecological imbalance [1–3]. Additionally, N_2O is recognized as a substance that depletes the stratospheric ozone layer, and anthropogenic N_2O emissions currently represent the largest source of ozone-depleting substances. N_2O emissions originate from multiple pathways, fuel combustion in industrial settings, agricultural activities, incineration, industrial combustion, and natural processes [4–6]. These emissions collectively exacerbate environmental challenges associated with N_2O , impacting both climate change and stratospheric ozone depletion. Quantitative measurement of N_2O concentrations is crucial for inverting N_2O emissions, which is essential for understanding and

mitigating its environmental impacts. Among various measurement approaches, optical methods stand out due to their high sensitivity and selectivity. In recent years, photoacoustic spectroscopy (PAS) has been widely applied in trace gas sensing owing to its advantages such as high sensitivity, wavelength independence, compact structure, and wide dynamic range [7–11].

In PAS based on photoacoustic cell (PAC), the efficiency of the photoacoustic generation is maximized when the modulation frequency $f < \tau^{-1}$, indicating that the modulation frequency must be lower than the relaxation rate of the target molecule within a given mixture. The modulation frequency is chosen to match the resonance of the acoustic cell, which is exploited to enhance the acoustic signal amplitude through the establishment of standing waves [12–15]. On the other hand, the relaxation rate depends on how efficient the energy transfer processes, i. e., vibrational-vibrational (V-V), vibrational-translational (V-T), and

^{*} Corresponding authors at: State Key Laboratory of Quantum Optics Technologies and Devices, Institute of Laser Spectroscopy, Shanxi University, Taiyuan 030006, China.

E-mail addresses: vincenzoluigi.spagnolo@poliba.it (V. Spagnolo), donglei@sxu.edu.cn (L. Dong), wuhp@sxu.edu.cn (H. Wu).

 $^{^{\}rm 1}$ These authors have contributed equally to this work

rotational-translational (R-T), occur through all the possible pathways offered by the collisional partners in the gas mixture. Consequently, the introduction of substances such as water vapor, oxygen, or carbon dioxide, or modifications to carrier gas matrices (e.g., sulfur hexafluoride and hydrogen) in PAS measurements [16,17], can modify energy transfer or energy level transitions of target gases, thereby affecting their relaxation pathways and photoacoustic responses [18,19]. Water vapor, for instance, possesses a high-density energy level structure, determining for many target molecules a significant acceleration of the energy relaxation and leading in turn to a more efficient photoacoustic generation [20–23].

In recent years, two main approaches have been implemented to model the effects of energy relaxation in photoacoustic detection, one relying on the evaluation of photoacoustic signal dependence on the matrix fluctuations through multivariate analysis of extended photoacoustic spectra [24], the second based on the implementation of the photoacoustic phase theory in digital twin modeling of the photoacoustic signal [25,26]. The relaxation dynamics of target gas molecules can be deduced from the phase characteristics of photoacoustic signal. Phase information is influenced by multiple factors, including geometric dimensions of the PAC, response time of the detection system, gas sample interactions with materials all along the gas line, thermodynamic and optical properties of the gas sample, energy level lifetimes of the non-radiative transition processes [27,28]. During measurements, the photoacoustic phase developed due to the gas delivery process becomes a constant of the system, while further modifications of this value can be addressed to variation of the thermodynamic properties and relaxation dynamics. This makes photoacoustic a valuable tool for measuring gas matrix-related physical quantities, such as relaxation rates. As first proposed by G. Gorelik in 1946, phase variations in the photoacoustic response as a result of a photoacoustic excitation can serve as a metric for measuring V-T relaxation rates [29]. The principle of photoacoustic detection involves target molecules absorbing optical radiation to transition from ground states to excited states, followed by energy recovery through V-T relaxation processes. Although V-T relaxation processes dominate, V-V energy transfer mechanisms cannot be neglected [30-32]. In many cases, it has been demonstrated that adding water vapor as a quencher to a mixture containing slow-relaxer target molecules improves radiation-to-sound conversion efficiency. Studying the photoacoustic response at different water vapor concentrations thus allows characterization of the relaxation dynamics of N2O in standard atmospheric air matrices, enabling the evaluation of relaxation rate values.

This study employed a 4.5 μm distributed feedback quantum cascade laser (DFB-QCL) and a custom-designed PAC to investigate the V-T

relaxation rates of N_2O (ν_3) under varying H_2O concentrations, with the aim of analyzing water vapor influence on photoacoustic detection processes and using the phase variations of photoacoustic signals to calculate the relaxation rate measurements.

2. Design of N2O sensor

2.1. Wavelength selection and high-power laser

In order to exploit the N_2O photoacoustic signal and phase to retrieve the relaxation rates, it is necessary to verify that no spectral interference occurs among the selected N_2O transition and all the atmospheric absorbers that can be found in the mixtures under investigation.

According to the HITRAN database, the absorbance of a mixture of 20 ppb of N₂O was simulated in the range 2213 cm⁻¹-2217 cm⁻¹ at 760 Torr, together with the main component of the air, namely carbon monoxide, carbon dioxide, methane, and water, at their typical atmospheric concentrations. The N₂O absorption line at 2215.06 cm⁻¹ is unaffected by interference from H₂O or other common atmospheric molecules within this spectral region, as illustrated in Fig. 1a. For this purpose, a high-power DFB-QCL designed by AdTech Optics was selected. The emission wavelength of the laser was characterized by using a wavemeter (Bristol Instruments, 671B-MIR) to identify the best operating conditions to reach the target absorption line. Based on the wavelength tuning coefficients, which are 0.013 cm⁻¹/mA for current and 0.21 cm⁻¹/°C for temperature, an operating temperature of 20 °C and a drive current of 530.1 mA were chosen to precisely match the target absorption line, as demonstrated in Fig. 1b. At this selected operating point, the output power of the QCL was approximately 45 mW after passing through the PAC.

2.2. Sensor architecture

The experimental setup is illustrated in Fig. 2. This study introduced the design of a custom-built PAC featuring two parallel tubular channels, each with a length of 90 mm and a diameter of 8 mm. The PAC was equipped with two CaF_2 windows, each measuring 25.4 mm in diameter. Two selective capacitive cylindrical microphones with identical frequency response and sensitivities were symmetrically mounted at the mid-point of each resonator. The continuous-wave DFB-QCL was employed as the excitation source for N_2O molecules. It was driven by a current controller (ILX Lightwave, Model LDX-3220) and stabilized by a temperature controller (Thorlabs, Model TED200C). A water-cooling system was incorporated to enhance heat dissipation efficiency. A function generator (Agilent, Model 33500B) generated sinusoidal wave

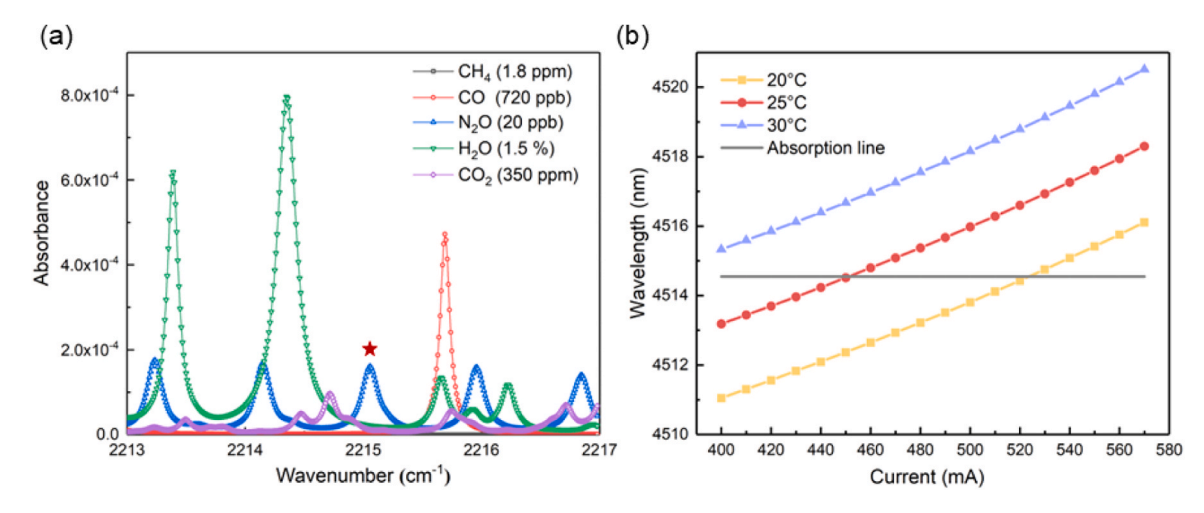


Fig. 1. (a) Simulated absorbance spectra for N_2O and other common atmospheric gases at 760 Torr. (b) Emission wavelength tuning of the DFB-QCL as a function of injection current and temperature.

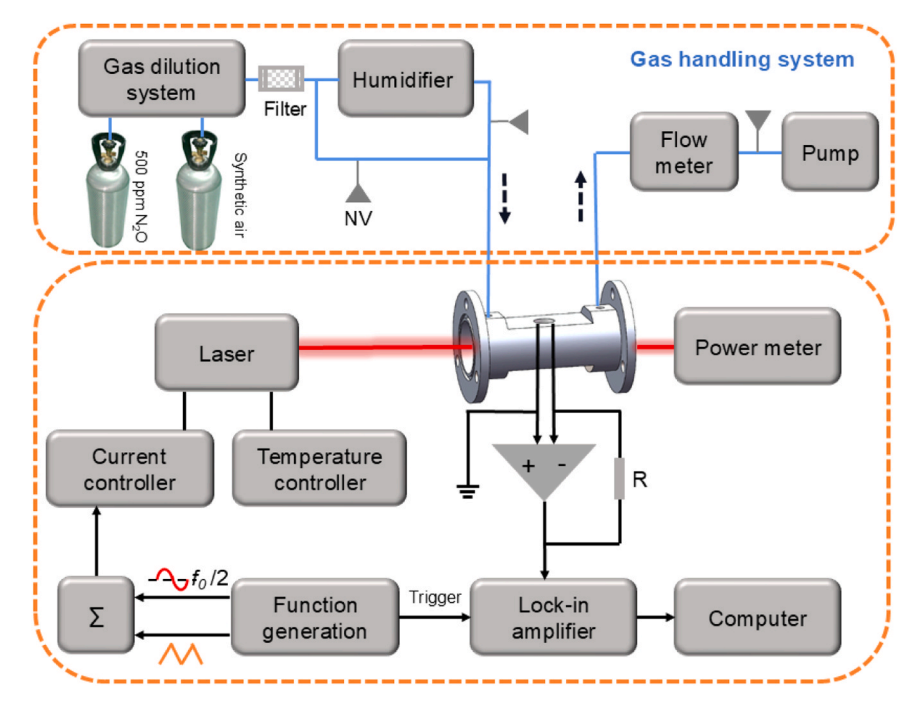


Fig. 2. Schematic diagram of the PAS experimental setup based on the PAC.

and 20 mHz ramp signals for implementing second harmonic wavelength modulation spectroscopy (2f-WM). The modulation frequency was set to half the PAC's resonant frequency ($f_0/2 = 889$ Hz). The signals from the function generator were combined using an adder before being fed into the laser current driver. The laser beam passed through the PAC, and its output power was monitored in real time using a power meter. The photoacoustic signals generated inside the PAC were detected by the embedded microphones and amplified by transimpedance amplifiers. The amplified signals were then transmitted to a Lock-in amplifier (LIA) (Stanford Research Systems, Model SR830) for 2 f demodulation. The TTL synchronization signal from the function generator served as the reference input for the LIA. The data were stored on a computer running a custom LabView program. In the gas dilution system, two cylinders were employed. One contained a certified 500 ppm N2O mixture in synthetic air, with a nominal concentration uncertainty of 0.5 %. The other contained pure synthetic air. An Environics gas mixer (Environics Inc., Model EN4000) was used to adjust the dilution ratio of N₂O in synthetic air and to control the gas flow. The output of the mixer was connected to a dryer to remove water vapor. Two needle valves were then adjusted to regulate the $\rm H_2O$ concentration. The downstream of the PAC was equipped with a needle valve, a flow meter, and a diaphragm pump to precisely control the gas flow and pressure inside the PAC. All experiments were performed at room temperature. Measurements were carried out under conditions of 760 Torr and 150 sccm.

2.3. Stability performance of the sensor

To thoroughly assess the performance of the $\rm N_2O$ detection sensor based on PAS technology, the sensor system was operated under atmospheric pressure and room temperature conditions. During the experiment, the gas dilution system was employed to precisely generate $\rm N_2O$ gas samples with concentrations ranging from 10 ppm to 100 ppm. Fig. 3a shows the 2f-profile and the calibration curves at different $\rm N_2O$ concentrations. Linear regression analysis on the calibration curve provided an R-square value of 0.99993, as shown in Fig. 3b, confirming

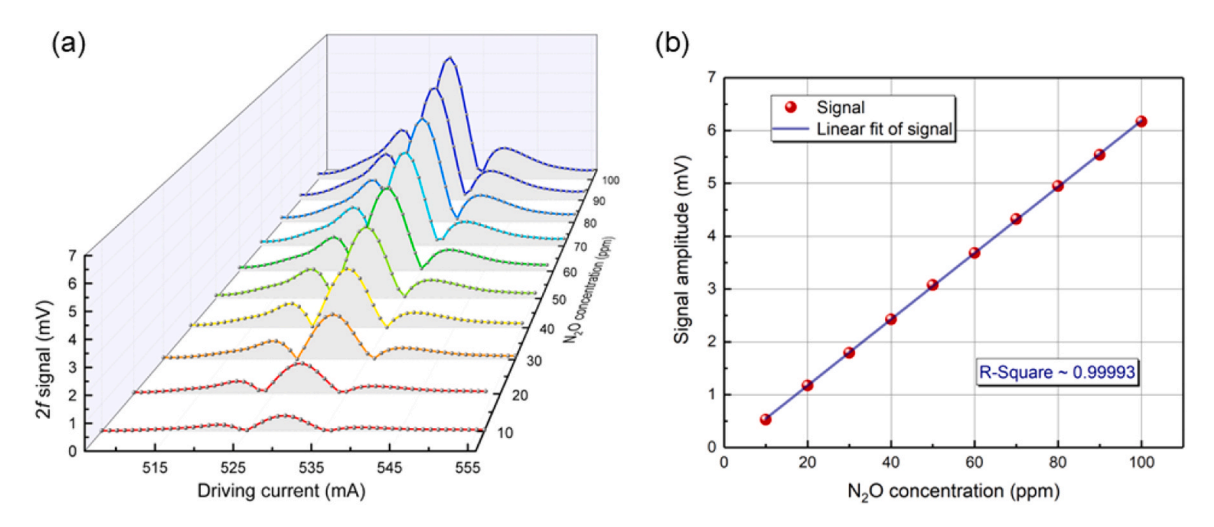


Fig. 3. (a) PAS-generated 2f signals for varying N_2O concentrations under 760 Torr and room temperature; (b) Linear correlation analysis between concentration and signal intensity.

the perfect linearity of the sensing system response at different $\rm N_2O$ concentrations. While the primary objective of this study is the validation of a novel method for measuring molecular relaxation times using the photoacoustic phase, the system's ultimate detection capabilities were also characterized. The detection limit for $\rm N_2O$ is 500 ppt with a 1 s integration time. Given that the typical concentration of $\rm N_2O$ in the ambient atmosphere is approximately 400 ppb, this system is fully capable of meeting the requirements for ambient atmospheric $\rm N_2O$ monitoring.

3. Molecule relaxation in the N2O-H2O-synthetic air system

As a linear triatomic molecule, N_2O exhibits three fundamental vibrational modes: the ν_1 symmetric stretching mode (1285 cm⁻¹, 7.8 μ m), the ν_2 bending mode (588.8 cm⁻¹, 17 μ m), and the ν_3 asymmetric stretching mode (2223.8 cm⁻¹, 4.5 μ m). Due to its asymmetric molecular structure, all three vibrational modes are infrared-active [40].

In the N_2O-H_2O -synthetic air system, the vibrational-to-translational (V–T) energy transfer of O_2 is relatively slow, causing excitation energy to accumulate in O_2 molecules and contributing negligibly to the photoacoustic signal. Moreover, the concentration of O_2 remains essentially constant, resulting in no significant impact on the relaxation process [18,36,41]. Therefore, the relaxation pathway of O_2 is generally not considered in the analysis, while the dominant role of H_2O is emphasized. The ν_3 absorption band of N_2O is centered at 2223.8 cm $^{-1}$. All related V–V and V–T relaxation pathways involving collisional partners are illustrated in Fig. 4. Dashed lines denote V–V energy transfer routes, whereas solid lines represent V–T relaxation channels. The corresponding rate constants are listed in Table 1.

The excited vibrational mode of N₂O (ν_3) initially absorbs laser energy, but the energy stored in the ν_3 band is unstable. It is primarily transferred to the ground state via V-T processes and dissipated to the ν_2 and ν_I modes through V-V processes. The relaxation time of the N₂O (ν_3) state can be expressed as:

$$\tau_{N_2O(\nu_3)}^{-1} = \tau_{V-T, N_2O(\nu_3)}^{-1} + \tau_{V-V, N_2O(\nu_3)}^{-1}
\tau_{V-T, N_2O(\nu_3)}^{-1} = p_{N_2O}k_{a1} + p_{H_2O}k_{a2} + p_{N_2}k_{a3}
\tau_{V-V, N_2O(\nu_3)}^{-1} = p_{N_2O}k_{V-V}$$
(1)

where p_{N_2O} , p_{H_2O} and p_{N_2} represent the partial pressures of 10–100 ppm N₂O (1 ×10⁻⁵-1 ×10⁻⁴ atm), 0–2.5 % H₂O (0–0.025 atm), and 78 % N₂ (0.78 atm) in a 1 atm gas mixture, respectively. The energy stored in the

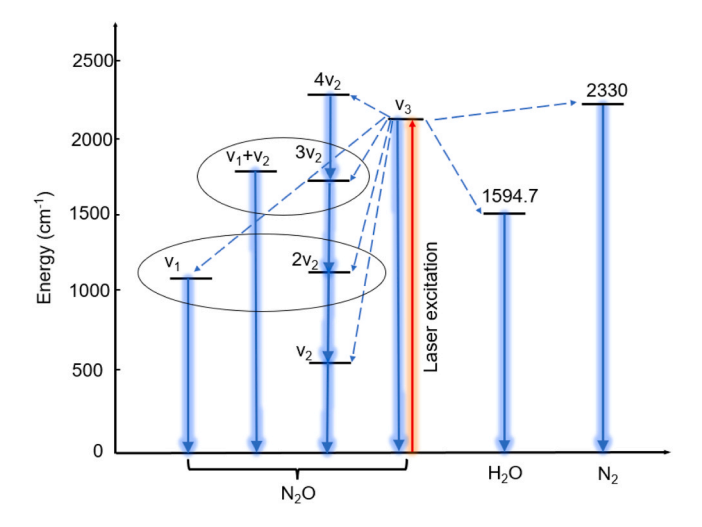


Fig. 4. Simplified schemes of the vibrational energy-level transfer diagrams for molecular systems.

Table 1Examples of relaxation rates of some vibrational states with different collisional partners.

Type	V-T	$rate (s^{-1} atm^{-1})$	ref
a	$N_2O (\nu_3) + N_2O \rightarrow N_2O + N_2O$	k _{a1}	[33]
		$\approx 5.426 \times 10^3$	
b	$N_2O (\nu_2) + N_2O \rightarrow N_2O + N_2O$	$k_{b1}\approx 7.7\times 10^5$	[34]
	$N_2O (\nu_2) + H_2O \rightarrow N_2O + H_2O$	$k_{b2}\approx 1.1\times 10^8$	[35]
	$N_2O(\nu_2) + N_2 \rightarrow N_2O + N_2$	$k_{b3}\approx 5.7\times 10^5$	[33]
c	$N_2O(\nu_1) + N_2O \rightarrow N_2O + N_2O$	$k_{c1}\approx 1.2\times 10^6$	[34],
			[35]
	$N_2O(\nu_1) + N_2 \to N_2O + N_2$	$k_{c3} < 10^5$	[35]
	$H_2O (\nu_2) + H_2O \rightarrow H_2O + H_2O$	$k_{22}\approx 2.7\times 10^7$	[36]
	$H_2O(\nu_2) + N_2 \rightarrow H_2O + N_2$	$k_{23}\approx 1.0\times 10^6$	[37]
	$N_2 + N_2 \rightarrow N_2 + N_2$	$k_{33}\approx 1.0\times 10^6$	[38]
Type	V-V	$rate (s^{-1} atm^{-1})$	ref
	$N_2O (\nu_3) + N_2O \rightarrow N_2O (4\nu_2) + N_2O$	1.83	[33]
	$N_2O (\nu_3) + N_2O \rightarrow N_2O (3\nu_2, \nu_1 + \nu_2)$	1.84	[39]
	$+ N_2O$		
	$N_2O (\nu_3) + N_2O \rightarrow N_2O (\nu_1, 2\nu_2) + N_2O$	1.88	[40]

 $N_2O(\nu_1)$ and $N_2O(\nu_2)$ states will ultimately be transferred via V-T processes under the influence of different collision partners. Specifically, these processes can be expressed as:

$$\tau_{V-T, N_2O(v_2)}^{-1} = p_{N_2O}k_{b1} + p_{H_2O}k_{b2} + p_{N_2}k_{b3}$$

$$\tau_{V-T, N_2O(v_1)}^{-1} = p_{N_2O}k_{c1} + p_{H_2O}k_{c2} + p_{N_2}k_{c3}$$
(2)

Therefore, in this N₂O-H₂O-synthetic air system, the total relaxation time τ for generating the PAS signal through three V-T processes (a, b, and c) can be generally described by the combined V-T relaxation of N₂O $(\nu_1, \nu_2, \text{ and } \nu_3)$. It is important to note that the V-V processes were omitted from the calculations due to their significantly smaller contribution compared to the dominant V-T processes. This simplification is strongly supported by the data in Table 1. We can observe that the primary V-T relaxation rates are exceptionally fast. For instance, for the $N_2O(\nu_2)$ mode, the V-T relaxation rate via collision with N_2O (k_{b1}) is approximately $7.7 \times 10^5 \, \text{s}^{-1} \, \text{atm}^{-1}$, the rate via collision with N_2 (k_{b3}) is approximately $5.7 \times 10^5 \, \text{s}^{-1} \, \text{atm}^{-1}$, and the rate via collision with H_2O (k_{b2}) is even higher, at 1.1×10^8 s⁻¹ atm⁻¹. In sharp contrast, the V-V energy transfer rates from $N_2O(\nu_3)$ listed in Table 1 (e.g., transfers to the $4v_2$ or $3v_2$ modes) are only 1.83, 1.84, and 1.88 s⁻¹ atm⁻¹, respectively. Therefore, this enormous discrepancy provides strong quantitative evidence that the contribution of V-V processes to the total systemic relaxation rate is indeed negligible. By incorporating the contributions of all relevant V-T relaxation pathways, the final calculated overall relaxation time of the system is about 2.7 μs atm. This result provides a comprehensive understanding of the energy dissipation mechanisms within the ternary gas mixture, highlighting the critical role of V-T interactions in determining the system's relaxation dynamics.

4. Influence of molecular relaxation in photoacoustic

In N₂O-H₂O-synthetic air gas mixtures, the energy transfer pathways from the excited N₂O (ν_3) state to relaxation processes are complex. This complexity necessitates the development of a simplified model to investigate the impact of H₂O on the overall relaxation time. Within the N₂O-synthetic air system, the relaxation process can be approximated as $\tau_1=1/k_1$, where k_1 represents the relaxation rate constant. The relatively long τ_1 observed in dry N₂O-synthetic air mixtures, characterized by low photoacoustic signal amplitudes, may stem from the inefficient vibrational relaxation of N₂O and partial energy transfer to N₂. This energy transfer results in metastable vibrationally excited N₂ states, which are characteristic of the N₂O-synthetic air system. In contrast, H₂O effectively promotes collisional energy exchange through V-T and V-V interactions with neighboring molecules, thereby acting as an efficient catalyst for molecular energy deactivation. In the simplified model,

the resonant energy transfer rate constant from the N_2O -synthetic air system to H_2O (V-V interaction) is denoted as k_2 , which is proportional to the H_2O concentration and the additional relaxation pathways introduced by H_2O (V-T interaction) are denoted as k_3 .

In a PAS system, the PA signal is generated by variations in gas pressure, which are proportional to the heat produced per unit volume during molecular vibrational energy relaxation. This relationship can be expressed as:

$$\frac{dP}{dt} = \frac{C}{nR} \frac{dH}{dt} \tag{3}$$

where C, n, and R represent the total heat capacity of the gas, the number of moles of gas, and the gas constant, respectively. In this system, the rate of heat production can be expressed as:

$$\frac{dH}{dt} = \Delta E(k_1 N + k_2 N + k_3 N^*) \tag{4}$$

where N is the number of excited molecules in the N_2O -synthetic air system. N^* represents the number of molecules excited by the addition of H_2O in the N_2O -synthetic air system. Hence, the relaxation pathways can be modelled by the following set of differential equations:

$$\frac{dN}{dt} = Z - k_1 N - k_2 N$$

$$\frac{dN^*}{dt} = k_2 N - k_3 N^* \tag{5}$$

where Z is the excitation rate of laser radiation, which can be expressed as: $Z=Z_0$ ($a+be^{i\omega t}$) , with the modulation frequency $\omega=2\pi f$. Therefore, the number of excited molecules N and N^* can be expressed as:

$$\mathit{N}(t) = Z_0 au_{12}$$
 ($a + rac{b}{\sqrt{1+\left(\omega au_{12}
ight)^2}}$) $e^{i(\omega t - arphi_{12})}$

$$N^*(t) = Z_0 \tau_{12} \tau_3 k_2 \left(a + \frac{b}{\sqrt{1 + (\omega \tau_{12})^2} \sqrt{1 + (\omega \tau_3)^2}} \right) e^{i(\omega t - \varphi_{12} - \varphi_3)}$$
 (6)

 $au_{12}=rac{1}{k_1+k_2}, \ arphi_{12}=\arctan\left(\omega au_{12}
ight)$ and $arphi_3=\arctan\left(\omega au_3
ight).$ Only the oscillating component of the pressure changes induced by the laser contributes to the measured photoacoustic signal. Using Eqs. (4), and (6), we can derive the general expression for the oscillating photoacoustic signal:

$$S(t) = \frac{S_0 \tau_{12}}{\sqrt{1 + (\omega \tau_{12})^2}} (k_1 + \frac{k_2}{\sqrt{1 + (\omega \tau_3)^2}} e^{-i\varphi_3}) e^{i(\omega t - \frac{\Pi}{2} - \varphi_{12})}$$
(7)

In this equation, the term $\pi/2$ represents the intrinsic phase difference between the periodic heat source and the resulting acoustic wave. In the PA effect, when the laser energy is absorbed by the molecules and converted into thermal energy in a sinusoidal manner, the generated sound pressure wave is proportional to the time derivative of this thermal energy. This indicates that the acoustic pressure signal leads the heat deposition process by $\pi/2$. To accurately measure the phase of the photoacoustic signal, it is necessary to determine the instrumental phase shift ϕ_0 introduced by the measurement system. As previously mentioned, the measurements were performed using wavelength modulation techniques and second harmonic detection. To determine the phase shift ϕ_0 of the optical input signal's second harmonic, direct absorption measurements were conducted using a high-concentration N2O gas mixture at the same pressure as the PAS measurements. The result of this measurement was $\phi_0=90.12^\circ$. Assuming that $E_1=k_1/\omega$ and φ_3 are constants, and $E_2x = k_2(x) / \omega$ is a function of H₂O concentration x, Eq. (7) yields the following expression for the PA signal amplitude as a function of *x*:

$$S(x) = S_0 \times \frac{\sqrt{E_1^2 + 2E_1E_2 \frac{1}{\sqrt{1 + \tan^2(\varphi_3)}} \cos(\varphi_3)x + \frac{1}{1 + \tan^2(\varphi_3)} E_2^2 x^2}}{\sqrt{1 + (E_1 + E_2 x)^2}}$$
(8)

The phase of the PA signal as a function of x is given by:

$$\varphi(x) = \phi_0 - \frac{\pi}{2}$$

$$-\arctan\left(\frac{1}{E_1 + E_2 x}\right) - \arctan\left(\frac{E_2 \sin(\varphi_3) x}{E_1 \sqrt{1 + \tan^2(\varphi_3)} + E_2 \cos(\varphi_3) x}\right)$$
(9)

5. Results and discussion

5.1. Consistency of resonance frequency in a PAC

The resonance frequency of the PAC is significantly dependent on the type of relaxing molecules. Previous studies have demonstrated that the introduction of molecules with different relaxation properties leads to shifts in the acoustic resonance characteristics [14]. Without dynamic calibration of the excitation frequency, the detection sensitivity decreases due to incomplete standing-wave field formation. In particular, during H2O concentration gradient experiments, the precise determination of the resonance frequency is an essential prerequisite for ensuring measurement accuracy. To quantify this effect, the laser was operated at a temperature of 20 °C and a drive current of 530.1 mA, maintaining precise locking to the characteristic absorption peak of N₂O. Gas samples were prepared through a flow controller and subsequently injected into the PAC for analysis. A frequency scanning system was implemented on the LabView virtual instrument platform to record the acoustic resonance response curve with a resolution of 0.3 Hz. As illustrated in Fig. 5, the addition of 2.5 % H₂O to 10 ppm N₂O samples resulted in an approximately 5-fold increase in signal amplitude compared to samples containing only 0.5 % H₂O. This result demonstrates the significant influence of H₂O on photoacoustic relaxation of N2O due to its rapid energy transfer dynamics. Although variations in photoacoustic phase may originate from resonance frequency drift, the experiments clearly showed that changes in water vapor concentration produced no observable effect on the intrinsic resonance frequency of the PAC. The invariance of the resonance frequency across different H_2O levels confirms the feasibility of employing photoacoustic phase analysis

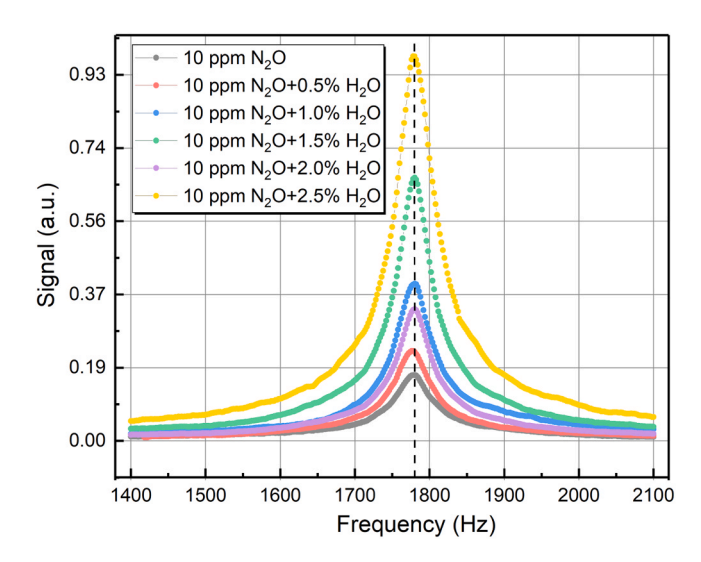


Fig. 5. Frequency response curve of the PAC as a function of the N_2O signal with the addition of different concentrations of H_2O .

for characterizing molecular relaxation times.

5.2. Amplitude and phase analysis

As illustrated in Fig. 6a, experiments observed the variation pattern of photoacoustic signal amplitude with H₂O concentration. With a fixed 1.5 % H₂O addition, the photoacoustic signal amplitude of 15 ppm N₂O was approximately five times that of 5 ppm N₂O, indicating that more N₂O molecules were influenced by the rapid relaxation effect of H₂O molecules. The vibrational relaxation process of N2O molecules was primarily dominated by the energy transfer mechanism of N2O-H2O collision pairs. The photoacoustic signal increased significantly when the H₂O concentration was changed from a dry mixture to a humidified mixture containing 2.5 % H₂O. The signal gains were 7.6, 8.6, and 7.3 for N₂O concentrations of 5 ppm, 10 ppm, and 15 ppm, respectively. This demonstrated that with appropriate H₂O addition, neither excessively high nor low N2O concentrations fully utilized the rapid relaxation effect of H₂O to enhance the photoacoustic signal. Theoretical models based on collision cross-sections predicted a saturation trend in signal intensity when added H2O exceeded a critical threshold. However, within the current concentration range (0-25000 ppm H₂O), no discernible inflection points or plateau trend was observed in the system. This suggests the potential presence of competitive mechanisms from alternative relaxation pathways, or that the concentration relationship between N2O and H2O in the experiment failed to reach the critical point where relaxation rates mutually compensated each other.

In terms of phase detection as shown in Fig. 6b, this study employs a differential phase measurement scheme, using the built-in reference signal of the LIA as a benchmark to obtain relative phase difference information. When conducting experiments, it is essential to fully consider the phase shift introduced by instruments and electronic equipment. The phase measured in this experiment is not an absolute value but a relative phase, which is determined under the condition of maintaining a constant reference phase of the LIA. The observed phase lag phenomenon mainly originates from the slow V-T relaxation process.

For different H_2O concentration conditions, we applied Eqs. (8), (9) to approximate the measured photoacoustic signal amplitude and phase. By fitting the experimental data with the theoretical trends obtained from the presented model, we determined the best-fit parameters, which in turn allowed us to determine the relaxation times of N_2O (τ_1) and H_2O (τ_3) molecules in gas mixture under atmospheric pressure and ambient temperature conditions. The phase shift ϕ_0 introduced by the measurement system was experimentally measured and found equal to 90.12° .

Eqs. (8) and (9), corresponding to the amplitude and phase, were used to define the three unknown quantities as A, B, and C. These were then substituted into the formulas, and polynomial data fitting was employed. After fitting as shown in Fig. 7a and b, the parameters obtained were able to satisfy both equations simultaneously, with specific parameter values of ($E_1=55.97$, $E_2=53.64$, $\varphi_3\approx 1.57$ rad). Finally, we calculated the relaxation times under normal pressure to be $\tau_1\approx 1.6~\mu s$ atm and $\tau_3\approx 0.33~\mu s$ atm. While a comprehensive and complete analysis of the relaxation processes of combination bands and overtone vibrational energy levels in this gas system would be extremely complex, the simplified relaxation model allows us to achieve a good fit with the measured amplitude and phase functions, with correlation coefficients of 0.998 and 0.997, respectively.

The relaxation time characteristics of gas molecules in photoacoustic effects are predominantly governed by molecular structural properties. Taking the polar molecule H₂O as an exemplary case, its permanent dipole moment (1.88 D) significantly enhances the probability of vibrational-rotational energy level transitions, thereby accelerating energy transfer rates and resulting in shorter relaxation times. When the light source modulation frequency is lower than the molecular characteristic relaxation velocity, energy absorption efficiency is substantially augmented, subsequently expediting the relaxation process. Notably, the introduction of H2O in gas mixtures creates new energy transfer pathways through its collision cross-section, thereby promoting the relaxation of N2O molecules. The concentration ratio within gas mixtures directly influences relaxation times by modulating effective collision cross-section parameters. These influencing factors operate synergistically rather than independently, collectively determining the relaxation time constants reflected in photoacoustic signals. When factoring in these known uncertainties and simplifications, the experimentally fitted value (1.6 μs atm) and the literature-based theoretical estimate (2.7 µs atm) are of the same order of magnitude and are numerically close. We argue that this correspondence strongly validates the reasonableness and efficacy of our proposed phase-measurement method and the simplified model used to interpret it. It is particularly noteworthy that the v_1 (<1 μ s atm) and v_2 energy levels of N₂O exhibit relatively faster V-T relaxation rates, a phenomenon primarily attributable to their specific energy transfer pathway configurations.

6. Conclusion

In conclusion, it is demonstrated in this study that PAS technique not only possesses high-precision gas concentration detection capabilities

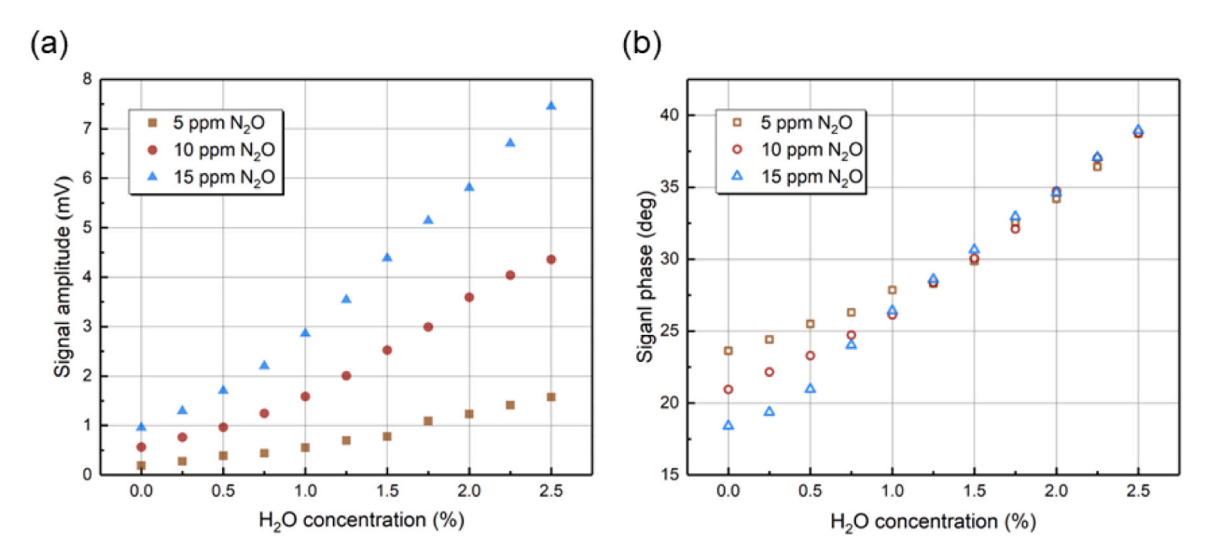


Fig. 6. (a) Signal amplitude of the N_2O -synthetic air mixture as a function of varying H_2O concentrations. (b) Signal phase of the N_2O -synthetic air mixture as a function of varying H_2O concentrations.

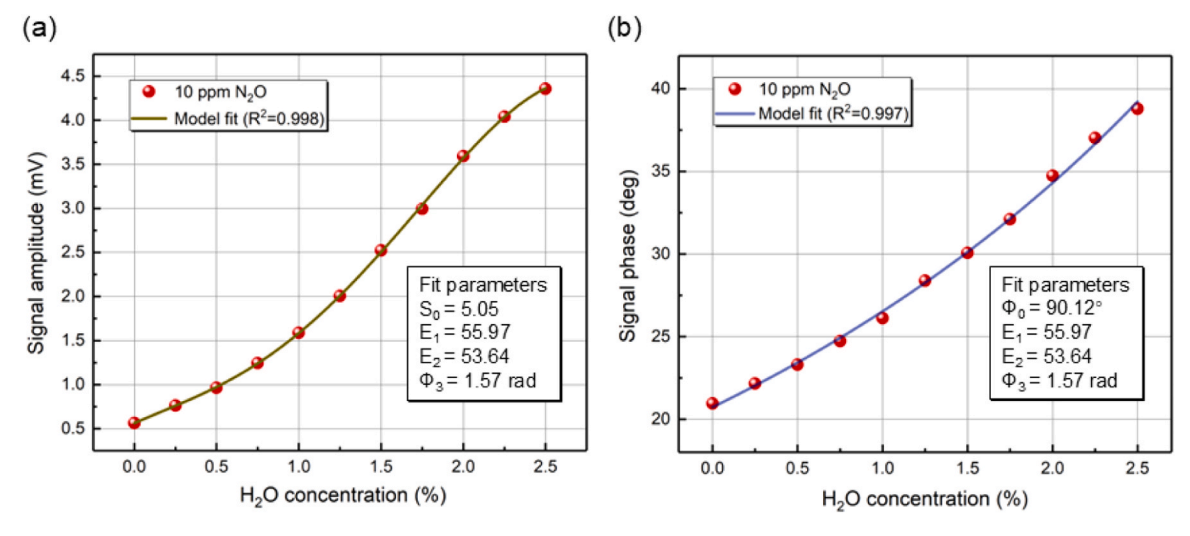


Fig. 7. (a) Signal amplitude of 10 ppm N₂O as a function of varying H₂O concentrations. (b) Signal phase of 10 ppm N₂O as a function of varying H₂O concentrations.

but also enables accurate calculation of gas relaxation times through phase characteristic analysis, showcasing its unique "concentration-relaxation" dual analytical functions. The relaxation dynamics of the ν_3 vibrational energy level of N_2O molecules in gas mixture was focused on, with a comprehensive theoretical model coupling V-V energy transfer and V-T relaxation processes being developed. By integrating this model with photoacoustic phase analysis methods, the first-ever extraction of N_2O (ν_3) vibrational relaxation time constants (1.6 μs atm) and H_2O relaxation times (0.33 μs atm) was achieved, which are in reasonable agreement with literature values. The findings fully substantiate that PAS phase-resolved technology is an advanced spectroscopic analysis method with both precision and reliability for measuring gas molecular energy relaxation rates, and its unique phase detection dimension opens new avenues for kinetic studies of complex systems.

CRediT authorship contribution statement

Ruyue Cui: Software. Jialiang Dai: Investigation. Gang Wang: Formal analysis. Jiapeng Wang: Data curation. Pietro Patimisco: Visualization. Angelo Sampaolo: Supervision. Mariagrazia Olivieri: Validation. Chaofan Feng: Methodology. Yong Wang: Writing – original draft. Lei Dong: Funding acquisition, Conceptualization. Vincenzo Spagnolo: Writing – review & editing. Hongpeng Wu: Writing – review & editing.

Declaration of Competing Interest

The authors declare that they have no known competing financial interests or personal relationships that could have appeared to influence the work reported in this paper.

Acknowledgments

The project is supported by National Natural Science Foundation of China (NSFC) (62475137, 62235010, 62105252, 62505163); Shanxi Provincial Special Fund for Scientific and Technological Cooperation and Exchange (202404041101022, 202304041101019); The Shanxi Science Fund for Distinguished Young Scholars (20210302121003); Fundamental Research Program of Shanxi Province, China (202403021212183); The Scientific and Technological Innovation Programs of Higher Education Institutions in Shanxi Province of China (2024L014).

Data Availability

Data will be made available on request.

References

- [1] Ya Li, Hanqin Tian, Yuanzhi Yao, Hao Shi, Zihao Bian, Yu Shi, Siyuan Wang, Taylor Maavara, Ronny Lauerwald, Shufen Pan, Increased nitrous oxide emissions from global lakes and reservoirs since the pre-industrial era, Nat. Commun. 15 (1) (2024) 942.
- [2] Jianxin Ma, Zhangxing He, Lei Dai, Yongguang Liu, Jing Zhu, Honghao Liu, Yuehua Li, Weiwei Meng, Ling Wang, Mixed potential sensor using YSZ and BaMoO₄-SE for detection of low concentrations N₂O, Sens. Actuators B Chem. (2025) 137798.
- [3] Yanbin Ren, Junya Du, Minghui Zhang, Jingsong Li, Laser absorption spectroscopy based on dual-convolutional neural network algorithms for multiple trace gases analysis, Sens. Actuators B Chem. 420 (2024) 136476.
- [4] Muhammad Rizwan, Hurain Tanveer, Muhammad Hayder Ali, Muhammad Sanaullah, Abdul Wakeel, Role of reactive nitrogen species in changing climate and future concerns of environmental sustainability, Environ. Sci. Pollut. Res. 31 (39) (2024) 51147–51163.
- [5] Huimin Han, Zeeshan Zeeshan, Bandeh Ali Talpur, Touseef Sadiq, Uzair Aslam Bhatti, Emad Mahrous Awwad, Muna Al-Razgan, Yazeed Yasid Ghadi, Studying long term relationship between carbon emissions, soil, and climate change: Insights from a global earth modeling framework, Int. J. Appl. Earth Obs. Geoinf. 130 (2024) 103902.
- [6] James Weber, James Keeble, Nathan Luke Abraham, David J. Beerling, Maria Val Martin, Global agricultural N₂O emission reduction strategies deliver climate benefits with minimal impact on stratospheric O₃ recovery, npj Clim. Atmos. Sci. 7 (1) (2024) 121.
- [7] Kumar Kinjalk, Francesco Paciolla, Bo Sun, Andrea Zifarelli, Giansergio Menduni, Marilena Giglio, Hongpeng Wu, Lei Dong, Diba Ayache, Davide Pinto, Aurore Vicet, Alexei Baranov, Pietro Patimisco, Angelo Sampaolo, Vincenzo Spagnolo, Highly selective and sensitive detection of volatile organic compounds using long wavelength InAs-based quantum cascade lasers through quartz-enhanced photoacoustic spectroscopy, Appl. Phys. Rev. 11 (2024) 021427.
- [8] Jiapeng Wang, Hongpeng Wu, Angelo Sampaolo, Pietro Patimisco, Vincenzo Spagnolo, Suotang Jia, Lei Dong, Quartz-enhanced multiheterodyne resonant photoacoustic spectroscopy, Light Science Applications 13 (1) (2024) 77.
- [9] Chu Zhang, Shunda Qiao, Ying He, Chaoming Liu, Yufei Ma, Multi-resonator T-type photoacoustic cell based photoacoustic spectroscopy gas sensor for simultaneous measurement C₂H₂, CH₄ and CO₂, Sens. Actuators B Chem. 427 (2025) 137168.
- [10] Raffaele De Palo, Annalisa Volpe, Pietro Patimisco, Andrea Zifarelli, Angelo Sampaolo, Antonio Ancona, Hongpeng Wu, Vincenzo Spagnolo, Femtosecond laser fabrication of black quartz for infrared photodetection applications, Light. Adv. Manuf. 6 (2025) 1–11.
- [11] Shunda Qiao, Ziting Lang, Ying He, Xiyang Zhi, Yufei Ma, Calibration-free measurement of absolute gas concentration and temperature via light-induced thermoelastic spectroscopy, Adv. Photonics 7 (2025) 066007.
- [12] Shuai Zhang, Yuan Cao, Chuan Li, Ruifeng Wang, Guishi Wang, Kun Liu, Xiaoming Gao, Sub-ppb level photoacoustic spectroscopy NOx sensor using a low cost 455 nm laser diode, Sens. Actuators B Chem. (2025) 138039.
- [13] Ke Chen, Nan Wang, Min Guo, Xinyu Zhao, Hongchao Qi, Chenxi Li, Guangyin Zhang, Lin Xu, Detection of SF₆ gas decomposition component H₂S based on fiber-optic photoacoustic sensing, Sens. Actuators B Chem. 378 (2023) 133174.
- [14] Hongming Yi, Olivier Laurent, Stephane Schilt, Michel Ramonet, Xiaoming Gao, Lei Dong, Weidong Chen, Simultaneous monitoring of atmospheric CH₄, N₂O, and

- H₂O using a single gas sensor based on Mid-IR quartz-enhanced photoacoustic spectroscopy, Anal. Chem. 94 (50) (2022) 17522–17532.
- [15] Kaiyuan Zheng, Wenxuan Luo, Lifu Duan, Shuangxiang Zhao, Shoulin Jiang, Haihong Bao, Hoi Lut Ho, Chuantao Zheng, Yu Zhang, Weilin Ye, Wei Jin, High sensitivity and stability cavity-enhanced photoacoustic spectroscopy with duallocking scheme, Sens. Actuators B Chem. 415 (2024) 135984.
- [16] Yingying Qiao, Liping Tang, Yang Gao, Fengtao Han, Chenguang Liu, Lei Li, Chongxin Shan, Sensitivity enhanced NIR photoacoustic CO detection with SF₆ promoting vibrational to translational relaxation process, Photoacoustics 25 (2022) 100334.
- [17] A.N. Starostin, I.V. Kochetov, A.K. Kurnosov, Yu.V. Petrushevich, M.D. Taran, Effect of quantum corrections for the increase in the gas density on the vibrational relaxation time, J. Exp. Theor. Phys. 137 (1) (2023) 23–29.
- [18] Max Müller, Thomas Rück, Simon Jobst, Jonas Pangerl, Stefan Weigl, Rudolf Bierl, Frank-Michael Matysik, An algorithmic approach to compute the effect of nonradiative relaxation processes in photoacoustic spectroscopy, Photoacoustics 26 (2022) 100371
- [19] Benjamin Lang, Philipp Breitegger, Georg Brunnhofer, Jordi Prats Valero, Simon Schweighart, Andreas Klug, Wolfgang Hassler, Alexander Bergmann, Molecular relaxation effects on vibrational water vapor photoacoustic spectroscopy in air, Appl. Phys. B 126 (2020) 1–18.
- [20] Bingyu Mo, Shanghu Zhou, Menglong Han, Pengsheng Xie, Chenxi Li, Xiao Han, Quanlei Qu, Jianwu Li, Ke Chen, Influence of water vapor concentration on photoacoustic spectroscopy-based characteristic gas analysis of transformer faults, Microw. Opt. Technol. Lett. 66 (7) (2024) e34258.
- [21] Ismail Bayrakli, A portable N₂O sensor based on quartz-enhanced photoacoustic spectroscopy with a distributed-feedback quantum cascade laser for medical and atmospheric applications, Opt. Quantum Electron. 53 (11) (2021) 642.
- [22] Yihua Liu, Haoyang Lin, Baiyang Antonio Zhou Montano, Wenguo Zhu, Yongchun Zhong, Ruifeng Kan, Bin Yuan, Jianhui Yu, Min Shao, Huadan Zheng, Integrated near-infrared QEPAS sensor based on a 28 kHz quartz tuning fork for online monitoring of CO₂ in the greenhouse, Photoacoustics 25 (2022) 100332.
- [23] Qian Wu, Haohua Lv, Leqing Lin, Hongpeng Wu, Marilena Giglio, Wenguo Zhu, Yongchun Zhong, Clamp-type quartz tuning fork enhanced photoacoustic spectroscopy, Opt. Lett. 47 (17) (2022) 4556–4559.
- [24] Aldo Francesco Pio Cantatore, Giansergio Menduni, Andrea Zifarelli, Pietro Patimisco, Marilena Giglio, Miguel Gonzalez, Huseyin R. Seren, Pan Luo, Vincenzo Spagnolo, Angelo Sampaolo, Methane, ethane, and propane detection using a Quartz-enhanced photoacoustic sensor for natural gas composition analysis, Energy Fuels 39 (2025) 638–646.
- [25] Andrea Zifarelli, Aldo Francesco Pio Cantatore, Angelo Sampaolo, Max Mueller, Thomas Rueck, Christine Hoelzl, Hubert Rossmadl, Pietro Patimisco, Vincenzo Spagnolo, Multivariate analysis and digital twin modelling: alternative approaches to evaluate molecular relaxation in photoacoustic spectroscopy, Photoacoustics 33 (2023) 100564.
- [26] Dragos C. Dumitras, Daniel C. Dutu, Catalin Matei, Alina M. Magureanu, Marius Petrus, Cristian Popa, Laser photoacoustic spectroscopy: principles, instrumentation, and characterization, J. Optoelectron. Adv. Mater. 9 (12) (2007) 3655–3660.
- [27] Gerard Wysocki, Anatoliy A. Kosterev, Frank K. Tittel, Influence of molecular relaxation dynamics on quartz-enhanced photoacoustic detection of CO_2 at $\lambda=2$ µm, Appl. Phys. B 85 (2006) 301–306.
- [28] András Miklós, Acoustic aspects of photoacoustic signal generation and detection in gases, Int. J. Thermophys. 36 (2015) 2285–2317.
- [29] Alexander A. Kosterev, Yuri A. Bakhirkin, Frank K. Tittel, Stefan Blaser, Yves Bonetti, Libor Hvozdara, Photoacoustic phase shift as a chemically selective spectroscopic parameter, Appl. Phys. B 78 (2004) 673–676.
- [30] Venedict A. Kapitanov, Boris A. Tikhomirov, Pulse photoacoustic technique for the study of vibrational relaxation in gases, Appl. Opt. 34 (6) (1995) 969–972.
- [31] Le Zhang, Lixian Liu, Xueshi Zhang, Xukun Yin, Huiting Huan, Huanyu Liu, Xiaoming Zhao, Yufei Ma, Xiaopeng Shao, T-type cell mediated photoacoustic spectroscopy for simultaneous detection of multi-component gases based on triple resonance modality, Photoacoustics 31 (2023) 100492.
- [32] Thomas G. Kreutz, Jack Gelfand, Richard B. Miles, Herschel Rabitz, A time domain photoacoustic study of the collisional relaxation of vibrationally excited H₂, Chem. Phys. 124 (3) (1988) 359–369.
- [33] David F. Starr, John K. Hancock, Vibrational deactivation of N_2O (001) by N_2O , CO, and Ar from 144 to 405 $^\circ$ K, J. Chem. Phys. 62 (9) (1975) 3747–3753.
- [34] Raymond T.V. Kung, Vibrational relaxation of the N_2O ν_1 mode, J. Chem. Phys. 63 (12) (1975) 5305–5312.
- [35] Raymond T.V. Kung, Vibrational relaxation of the N_2O ν_1 mode by Ar, N_2 , H_2O , and NO, J. Chem. Phys. 63 (12) (1975) 5313–5317.
- [36] Natalia Barreiro, Alejandro Peuriot, Gabriela Santiago, Vladimir Slezak, Water-based enhancement of the resonant photoacoustic signal from methane–air samples excited at 3.3 μm, Appl. Phys. B 108 (2012) 369–375.
- [37] Patrick L. Meyer, Manfred W. Sigrist, Atmospheric pollution monitoring using CO₂: laser photoacoustic spectroscopy and other techniques, Rev. Sci. Instrum. 61 (7) (1990) 1779–1807.
- [38] Henry E. Bass, Hans-Joachim Bauer, Kinetic model for thermal blooming in the atmosphere, Appl. Opt. 12 (7) (1973) 1506–1510.

- [39] John C. Stephenson, C.Bradley Moore, Temperature dependence of nearly resonant vibration-vibration energy transfer in CO₂ mixtures, J. Chem. Phys. 56 (3) (1972) 1295–1308
- [40] Richard D. Bates Jr., George W. Flynn, Arthur M. Ronn, Laser-induced vibrational fluorescence in nitrous oxide, J. Chem. Phys. 49 (3) (1968) 1432–1433.
- [41] Max Müller, Stefan Weigl, Jennifer Müller-Williams, Matthias Lindauer, Thomas Rück, Simon Jobst, Rudolf Bierl, Frank-Michael Matysik, Comparison of photoacoustic spectroscopy and cavity ring-down spectroscopy for ambient methane monitoring at Hohenpeißenberg, Atmos. Meas. Tech. 16 (18) (2023) 4263–4270.



Yong Wang is now pursuing a Ph.D. degree in atomic and molecular physics in the Institute of Laser Spectroscopy of Shanxi university, China. Her research interests include gas sensor and atmospheric detection.



Jiapeng Wang is now pursuing a Ph.D. degree in atomic and molecular physics in the Institute of Laser Spectroscopy of Shanxi university, China. Her research interests include optical sensors and photoacoustic spectroscopy.



Gang Wang is now pursuing a Ph.D. degree in atomic and molecular physics in the Institute of Laser Spectroscopy of Shanxi university, China. Her research interests include gas sensor and laser spectroscopy techniques.



Jialiang Dai received his master's degree from Hebei University, China, in 2024. He is now pursuing his Ph.D. at the Institute of Laser Spectroscopy, Shanxi University, China. His research interests include optical gas sensors, photoacoustic spectroscopy, light-induced thermoelastic spectroscopy and other laser spectroscopy.



Ruyue Cui received her dual Ph.D. degrees in physics from Shanxi University, China, and Université du Littoral Côte d'Opale, France, in 2023. Currently, she is a lecturer at the Institute of Laser Spectroscopy at Shanxi University. Her research interests encompass optical sensors and laser spectroscopy techniques.



the July 2013 issue.

Pietro Patimisco obtained the Master degree in Physics (cum laude) in 2009 and the Ph.D. Degree in Physics in 2013 from the University of Bari. Since 2018, he is Assistant professor at the Technical University of Bari. He was a visiting scientist in the Laser Science Group at Rice University in 2013 and 2014. Dr. Patimisco's scientific activity addressed both micro-probe optical characterization of semiconductor optoelectronic devices and optoacoustic gas sensors. Recently, his research activities included the study and applications of trace-gas sensors, such as quartz-enhanced photoacoustic spectroscopy and cavity enhanced absorption spectroscopy in the mid infrared and terahertz spectral region, leading to several publications, including a cover paper in Applied Physics Letter of



Chaofan Feng received his dual Ph.D. degrees in physics from Shanxi University, China, and Politecnico di Bari, Italy, in 2025. Currently, he is a lecturer at college of physics and electrical engineering at Shanxi University. His research interests include gas sensors, photoacoustic spectroscopy, and laser spectroscopy techniques.



Vincenzo Spagnolo obtained the Ph.D. in physics in 1994 from University of Bari. From 1997–1999, he was researcher of the National Institute of the Physics of Matter. Since 2004, he works at the Technical University of Bari, formerly as assistant and associate professor and, starting from 2018, as full Professor of Physics. Since 2019, he is vice-rector of the Technical University of Bari, deputy to technology transfer. He is the director of the joint-research lab PolySense between Technical University of Bari and THORLABS GmbH, fellow member of SPIE and senior member of OSA. His research interests include optoacoustic gas sensing and spectroscopic techniques for realtime monitoring. His research activity is documented by more than 220 publications and two filed patents. He has given more

than 50 invited presentations at international conferences and workshops.



Mariagrazia Olivieri obtained the M.S. degree (cum laude) in Physics in 2021 from the University of Bari. Since October 2021, she is a Ph.D. student at the Physics Department of the University of Bari carrying out her research work at PolySense Lab, joint-research laboratory between Technical University of Bari and THORLABS GmbH. Currently, her research activities are focused on the development of gas sensors based on Quartz Enhanced Photoacoustic spectroscopy for the analysis of com plex gas mixtures.

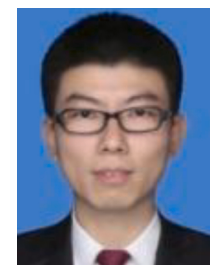


Lei Dong received his Ph.D. degree in optics from Shanxi University, China, in 2007. From June, 2008 to December, 2011, he worked as a post-doctoral fellow in the Electrical and Computer Engineering Department and Rice Quantum Institute, Rice University, Houston, USA. Currently he is a professor in the Institute of Laser Spectroscopy of Shanxi University. His research activities research activities are focused on research and development in laser spectroscopy, in particular photo-acoustic spectroscopy applied to sensitive, selective and real-time trace gas detection, and laser applications in environmental monitoring, chemical analysis, industrial process control, and medical diagnostics. He has published more than 100 peer reviewed papers with> 2200 positive citations.



Angelo Sampaolo obtained his Master degree in Physics in 2013 and the Ph.D. Degree in Physics in 2017 from University of Bari. He was an associate researcher in the Laser Science Group at Rice University from 2014 to 2016 and associate researcher at Shanxi University since 2018. Since May 2017, he was a Post-Doctoral Research associate at University of Bari and starting from December 2019, he is Assistant Professor at Polytechnic of Bari. His research activity has included the study of the thermal properties of heterostructured devices via Raman spectroscopy. Most recently, his research interest has focused on the development of innovative techniques in trace gas sensing, based on Quartz-Enhanced Photoacoustic Spectroscopy and covering the full spectral range from near-IR to

THz. His achieved results have been acknowledged by a cover paper in Applied Physics Letter of the July 2013 issue.



Hongpeng Wu received his Ph.D. degree in atomic and molecular physics from Shanxi university, China, in 2017. From 2015–2016, he studied as a joint Ph.D. student in the electrical and computer engineering department and rice quantum institute, Rice University, Houston, USA. Currently he is a professor in the Institute of Laser Spectroscopy of Shanxi University. His research interests include optical sensors and laser spectroscopy techniques.